EXPLORATION OF THE AIRBUS "NAUTILIUS" ENGINE INTEGRATION CONCEPT

Ludovic Wiart*, Camil Negulescu**
***ONERA, F-92190 Meudon, France, **Airbus Operations SAS, F-31060 Toulouse, France**

Keywords: *aerodynamics, propulsion, boundary-layer ingestion*

Abstract

The search for reduced fuel consumption of future transport aircraft involves an improvement of the propulsive efficiency. The current trend for engines is toward lower fan pressure ratio (and higher bypass ratio), which has to be compensated by larger mass flow rate. To deliver this increased mass flow rate, the fan diameter must be larger, making the integration of such engines on conventional aircraft a challenge. In parallel, boundary layer ingestion aircraft concepts are studied to further increase the aero-propulsive efficiency. The Airbus "Nautilius" concept [1] provides a solution for integrating high BPR engines and at the same time taking fully benefit of boundary-layer ingestion (BLI) for maximizing the aero-propulsive efficiency. This paper presents the results of a study conducted by ONERA on behalf of and in collaboration with Airbus to aerodynamically design and assess the performance of such a configuration.

1 Context and Objectives

In the frame of a previous project focusing on UHBR turbofan engines integration, ONERA developed the NOVA configurations [2] as an alternative to current single-aisle medium-haul aircraft. The considered mission is to carry 180 passengers (with a two-class layout) at a cruise Mach number of 0.82 for a 3000 nautical miles flight.

The challenges of performance assessment in presence of BLI were investigated on a configuration with engines buried on the rear side of fuselage and ingesting approximately 40% of fuselage boundary layer (Fig. 1). Among the advantages of, even partially, embedding the engine into the fuselage, savings in fuel (due to reduced jet/wake losses and wetted area) and weight are expected. In order to quantify the BLI benefits, a reference configuration with podded engines was developed as well (Fig. 1). A power saving of 5% in favor of the BLI configuration was exhibited in cruise condition [3].

Fig. 1. NOVA "BLI" & "Podded" configuration

The idea behind the Nautilius concept (Fig. 2, [1]) is to maximize the portion of ingested fuselage boundary layer while limiting the

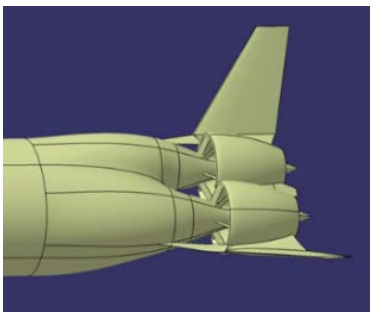
Fig. 2. Nautilius engine integration concept

azimuthal flow distortion at fan face by positioning the engines at the most downstream location possible and integrating them completely into the fuselage rear end.

In order to take advantage of the pre-existing NOVA "Podded" reference configuration, it was decided to investigate the Nautilius concept as a NOVA derivative by modifying solely the NOVA configuration aircraft rear end (common wings, common fuselage) (Fig. 3). For simplification, the tails have been omitted in the present study.

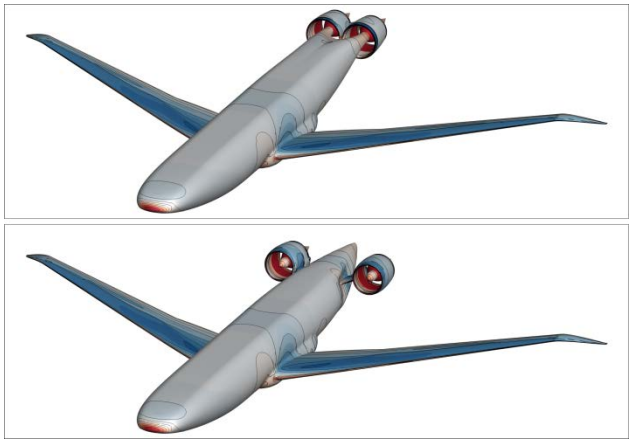

Fig. 3. Nautilius (top) VS Reference "podded" configuration (bottom) - without empennage

The results of the study conducted by ONERA on behalf of and in collaboration with Airbus to aerodynamically design and assess the performance of the Nautilius concept are presented in this paper.

First the main phenomena describing the benefits of BLI propulsion are recalled, followed by the description of the key design features of the Airbus Nautilius engine installation concept.

An axisymmetric study is then presented, which permitted to identify the main concept design parameters and to perform additional aerodynamic studies for the purpose of BLI propulsion understanding.

Finally, the 3D aerodynamic design and evaluation of the Nautilius rear end concept is shown.

2 Benefits of BLI Propulsion

In a classic aircraft configuration with podded engines (see Fig. 4), the airframe produces a deficit of streamwise momentum (the wake) while the engines produce an excess of velocity (the jet) to compensate it. The wake, as well as the jet, will then be dissipated by viscous effects downstream of the aircraft, and be accounted as losses. The classic decomposition (drag and thrust) of the forces acting on the airframe and the engine is possible in that case. A power balance [4] or exergy analysis [5] would however point out which portion of the kinetic energy from the wake could be recovered.

Wake ingestion, and by extension boundary layer ingestion, offer a potential of aeropropulsive efficiency improvement. This has been thoroughly described in the literature [6]. In an ideal scenario, the engine is placed downstream of the airframe (see Fig. 5) and re-energizes its wake by just the right amount to compensate the streamwise momentum deficit without any excess (jet). The commonly used metric to quantify those gains is the power-saving coefficient (PSC) which can be expressed as

$$PSC = \frac{P_{Podded} - P_{BLI}}{P_{Podded}} \qquad (1)$$

with P_{Podded} the fan power calculated for the "podded" configuration and P_{BLI} the fan power of the "BLI" configuration calculated at the same streamwise net force.

A classic drag/thrust breakdown is not possible in that case, and the exergy approach brings more insight on the loss sources and opportunities for configuration improvement.

As a negative side effect, BLI propulsion requires a more robust fan design from an aerodynamic and structural point of view in order to cope with the incoming distorted boundary layer flow. This brings potential additional performance and mass penalties, and therefore a BLI fan optimization need.

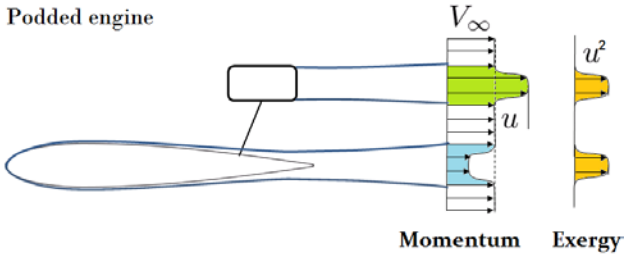

Fig. 4. Conventional podded-engine configuration [5]

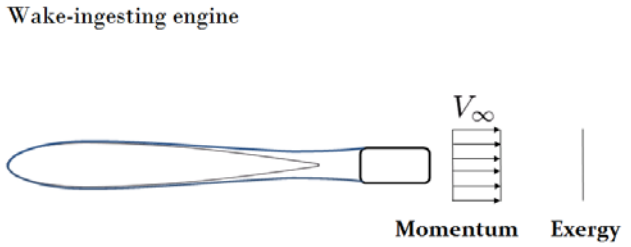

Fig. 5. Unconventional wake-ingesting configuration [5]

3 Airbus Nautilius concept presentation

3.1 Interest of Nautilius configuration

The so-called "Nautilius" aircraft concept developed by Airbus is built of two UHBR engines integrated on two distinct parts of converging diameter of a split fuselage rear end. The interest of this engine installation concept consists in the fact that it permits to ingest 100% of the aircraft fuselage boundary layer with an in-coming engine fan flow of limited azimuthal distortion. It allows therefore to take full benefit of the BLI propulsion, while limiting its drawbacks, like fan efficiency and fan mass penalties of a fan designed to work in a highly distorted boundary layer flow. Moreover, the Nautilius concept allows to install UHBR engine on the aircraft, adding thus the benefits of BLI and UHBR engine propulsion with the objective to fully optimize the propulsive efficiency. Propulsive efficiency levels of up to 90% can be targeted by such a concept, as high as CROR propulsion allows, but with limited drawbacks. Thus compared to CROR propulsion, for the same level of achievable propulsive efficiencies, the Nautilius concept permits to have engines of smaller size, less mass, reduced complexity, lower acoustic impact and permits to travel at higher speeds.

When compared to a conventional under-wing UHBR engine (15-BPR) aircraft installation, the Nautilius concept has a clear benefit in terms of propulsive efficiency and A/C drag, estimated to have an impact on fuel burn superior to 10%. The somewhat higher complexity with respect to a conventional A/C configuration (rear end mass impact, fan efficiency impact, shielding needs) has to be reduced by an intelligent engine-to-aircraft integration effort, in order to keep the resulting overall fuel burn benefit as high as possible.

Table 1 summarizes a high level comparison of an UHBR under-wing aircraft configuration, a CROR pusher SFN (Side Fuselage Nacelle) configuration and the Nautilius UHBR rear end BLI concept.

	Mach	ηprop	mass	noise	complexity
CROR	0.75	+8-10%	☹	☹	☹
UHBR	0.82	REF.	☺	☺	☺
Nautilius	0.82	+8-10%*	😐	😐	😐

* additional benefits are expected on A/C drag

3.2 Nautilius engine installation concept

The Nautilius aircraft concept consists of a conventional aircraft with the fuselage rear end split, downstream of the rear pressure bulkhead, into two parts of converging diameter as depicted in Figure 6.

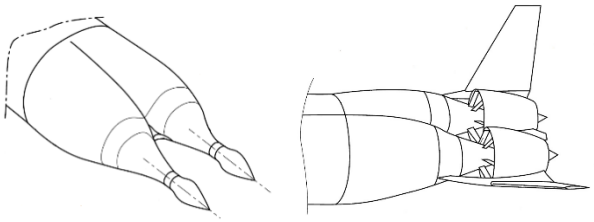

Fig. 6. Nautilius rear end concept [1]

On these two distinct fuselage parts, two fan module units with their nacelles are installed. The fan can be propelled by an electric motor or a turbomachinery, these power units are preferably placed upstream of the fan unit (Fig. 7) in order to avoid to place too much weight at the aircraft most aft position and thus trim drag penalties and rear end structural reinforcement needs.

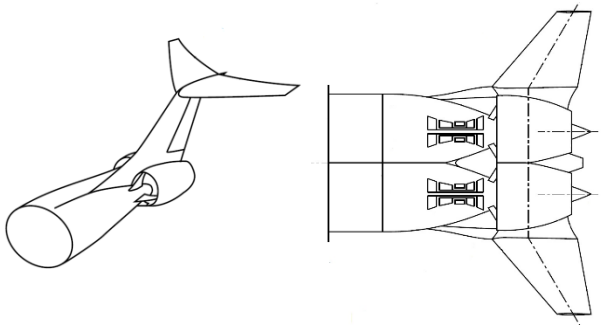

Fig. 7. Nautilius concept – design description

A certain amount of core engines shielding is required, at least for the LP and HP compressors, in order to be compliant to the 1/20 UERF hazard ratio in case of a compressor, turbine or fan disk burst.

Different tail configurations can be integrated, like V-tail (Fig. 6) and T-tail configurations (Fig. 7). The engines' vertical position is defined by the requirement of an acceptable take-off aircraft rotation angle, as shown in Figure 8.

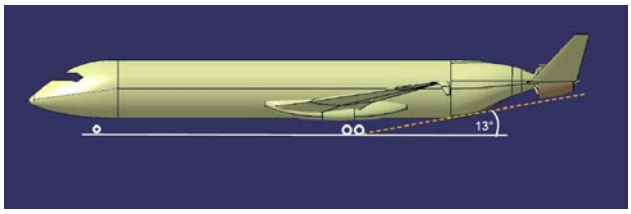

Fig. 8. Nautilius concept – take-off rotation angle

The Nautilius concept permits to integrate UHBR engines of 13-18 BPR.

4 2D-axisymmetric study

The objective of the 2D-axisymmetric study was to design the baseline engine aerolines of the Nautilius concept, i.e. engine inlet, exhaust and nacelle aerolines, on a simplified geometry permitting multiple low cost CFD iterations. Additionally, the 2D-axi study permitted to perform several trades for BLI understanding purposes.

4.1 Fan modeling

A NOVA dedicated fan was designed at ONERA through steady mixing plane calculations, using the elsA software (ONERA-Airbus-Safran property) [7]. It has 18 blades and delivers a fan pressure ratio (FPR) of 1.4 at design point, with a corrected specific mass flow at rotor plane of 209 kg/s/m². However, in order to perform multiple design iterations, a simplified fan model was required.

The fan stage model used for CFD should answer to two different requirements:

- to be able to reproduce the physical action of a fan (and OGV) on the incoming flow to provide reliable PSC data at a low computational cost;
- to be as close as possible to the 3D fan in terms of stagnation pressure and temperature jumps, mass flow rate, traction and power.

Good candidates are the Actuator Disk (AD) and body-force (BF) formulations.

Two AD models are available in the elsA software. The "helicopter" formulation has been ruled out for aeropropulsive performance assessment of BLI configurations [3]. The "propeller" formulation, despite its limitations in terms of numerical robustness, exhibited a more physical behavior and was used to generate most of the results presented in this paper.

A body-force modeling approach also implemented in elsA was used afterwards to confirm the trends obtained with AD. It consists in replacing the bladed region by an axisymmetric volume where source terms are applied in order to reproduce fan stage effects. In order to define the applied source terms, the body-force formulation of Hall (2015) improved by Thollet et al. (2017) has been used. Additional information regarding the implementation of the methodology is available in [9]. In short, in addition to blockage effects, body-forces are imposed in the right hand side of the Navier-Stokes equations. In the different flow tube planes from the blade hub to the tip (i.e. defined by an absence of force components normal to the plane), the body-forces can be decomposed in two components:

$$f_n = \frac{w^2}{2bh} 2\pi\delta \times \begin{cases} \frac{1}{\sqrt{1-M_r^2}} \; if M_r < 1 \\ \frac{2}{\pi\sqrt{M_r^2-1}} \; if \; M_r > 1 \end{cases}$$, which is perpendicular to the flow relative velocity $\vec{w}$ and serve to reproduce the main deviation and loading effects and:

$f_p = \frac{w^2}{2bk} K_{p0}$, which is this time parallel to the flow relative velocity $\vec{w}$ and is used to add losses. In the last two equations:

- $b = 1 - e/h$ is the blockage factor (where e is the axial thickness and h is the blades staggered spacing.
- M_r is the flow relative Mach number (i.e. relative to the rotating frame).
- δ is the flow deviation based on the blade profile: $\sin\delta = (\vec{w} \cdot \vec{n})/w$, in which $\vec{n}$ is the blade profile normal.
- $K_{p0} = 2 \times 0.0592 \times Re_{xc}^2$ is the friction drag coefficient and depends on the local Reynolds number Re_{xc} which is based on the whordwise position x_c on the blade.

The formulation as used in this study exclusively depends on the blade geometry and does not depend on calibration parameters. It is therefore quite convenient and straightforward to use for rapid airframe – fan coupling assessment.

4.2 Reference nacelle design

A reference isolated nacelle was designed as a derivative from the NOVA nacelle for a high bypass ratio fan diameter. The hub-to-tip ratio was increased from 0.25 to 0.34 to take into account the absence of the core flow.

AD lookup tables were generated with a predesign tool based on Glauert theory for propellers. CFD calculations were then performed using the elsA software with those lookup tables as inputs. A few iterations were necessary on both the fan model obtained and the fan nozzle exit area to obtain both the desired FPR and a realistic Mach number at fan face (M~0.6) at design point (see Fig. 9).

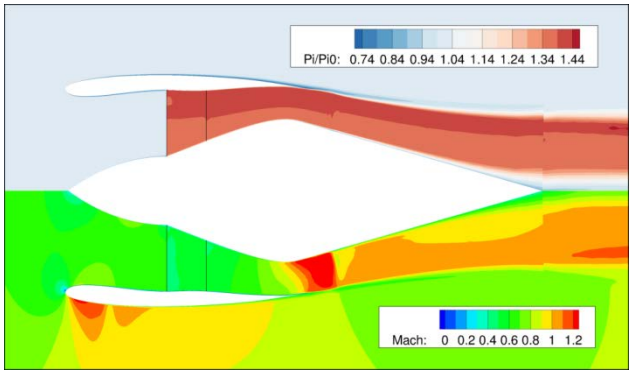

Fig. 9. Nautilius isolated nacelle at design point with actuator disk boundary conditions, Mach and stagnation pressure ratio fields

In order to limit the risk of flow separation downstream of the AD, the radial distribution of pressure ratio jump was voluntarily made more uniform than that of an actual fan. The swirl generated by the fan was accounted for, and a new development was implemented in elsA in order to mimic the stator effect with an AD too.

In order to simulate different engine regimes, the predesign software was then run with the obtained fan blade "geometry" at 90%, 70% and 40% of the nominal regime to obtain the corresponding lookup tables.

4.3 Nautilius axisymmetric body design

Although the Nautilius concept has two engines mounted at the rear of a single fuselage, an axisymmetric configuration is still relevant to evaluate the impact of a few parameters with relatively low geometry/mesh generation effort. A Nautilius axisymmetric body (see Figure 10) was therefore designed with roughly the overall dimensions of a short-medium range aircraft fuselage.

Fig. 10. Nautilius axisymmetric body

Compared to the reference isolated nacelle, the air inlet had to be modified to adjust to the local flow angle due to the rear fuselage shrinkage. The aerodynamic behavior at cruise conditions was investigated at different thrust levels (see Figure 11). From a purely aerodynamic point of view, at least for these zero angle-of-attack/zero

sideslip conditions, it was found that an aggressively short nacelle cowl (L/D~0.25) led to a satisfactory behavior of the inlet throughout the studied regimes. This can be explained by the fuselage section reduction upstream of the engine that acts as a diffuser for the incoming flow, which could be enough to bring it to the desired Mach number at fan face. However, for acoustic and structural reasons, the nacelle length-to-diameter ratio was set to 0.5.

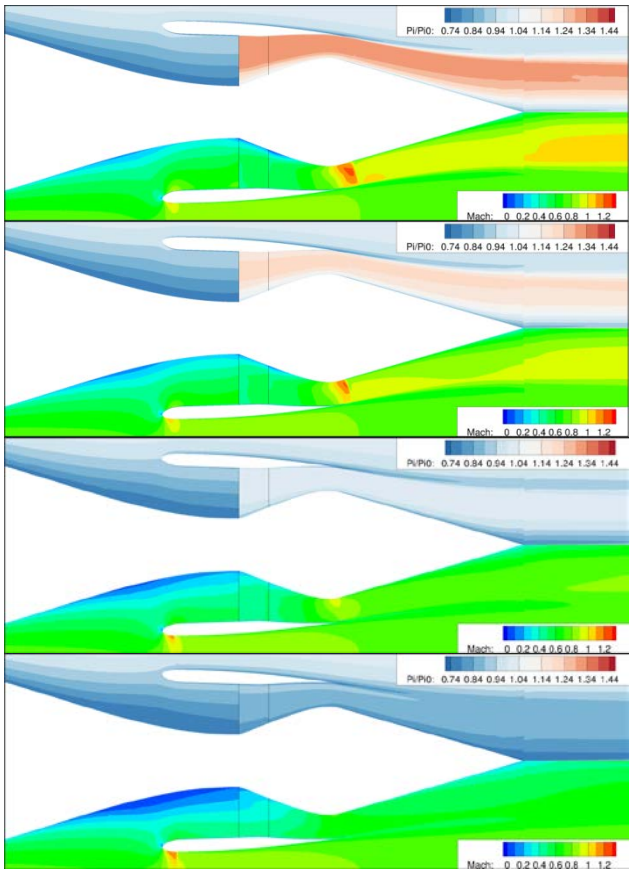

Fig. 11. Mach and stagnation pressure ratio fields for different engine regimes (from top to bottom: N=100%, N=90%, N=70%, N=40%) at cruise M=0.82

The air intake creates an adverse pressure gradient on the fuselage boundary layer, whose magnitude increases when the engine mass flow rate decreases. A separation appears upstream of the fan at N=40%, however this condition corresponds to a windmill condition (i.e. a fan power close to zero). At higher fan rotational speeds, the inlet performs well at the cruise Mach number. High power take-off simulations also permitted to verify the robustness of the inlet to stagnation point locations outside the highlight (see Figure 12).

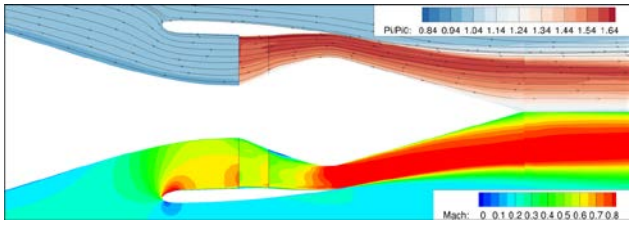

Fig. 12. Mach and stagnation pressure ratio fields in conditions representative of take-off, M=0,2

4.4 BLI and installation effect

To be able to evaluate a BLI gain on the axisymmetric Nautilius configuration, a reference non-BLI configuration was required. Therefore, a reference isolated fuselage was designed and its drag value added to that of the isolated nacelle.

Three different configurations were thus available for comparison (see Fig. 14):

- the isolated nacelle and fuselage (equivalent to a nacelle positioned infinitely away from the fuselage)
- the fuselage with the nacelle positioned downstream (far enough not to disturb the rear fuselage pressure field) in an academic “RAPRO2 like” manner [8]
- the installed configuration (iso wetted area vs configurations 1 & 2)

NB: To limit the geometric discrepancies between those configurations, the fan diameter, the nacelles length-to-diameter ratio and fan nozzle exit area are kept constant

Those calculations were carried out with both AD and BF fan stage models. For this latter, the Hall-Thollet model was used [9], which requires a rotor and stator geometry. Calculations were then performed by only specifying the RPM.

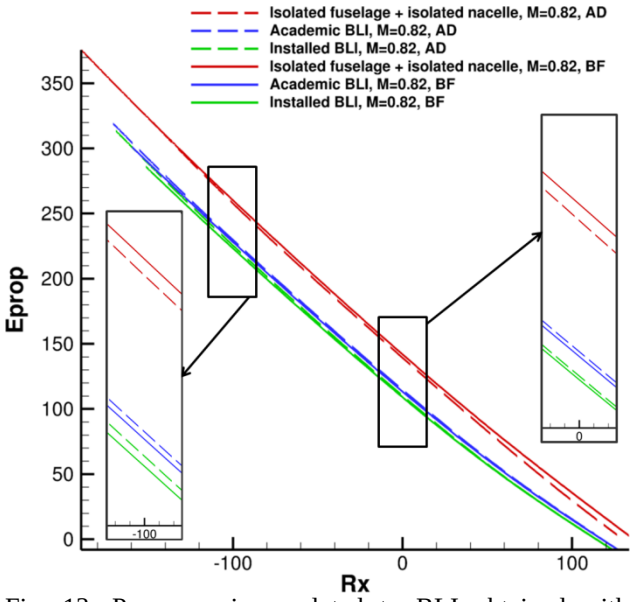

Fig. 13. Power savings related to BLI obtained with actuator disk and body force fan models

$$R_x = \frac{F_x}{0.5\rho_\infty V_\infty^2 A_{ref}} \qquad (2)$$

$$E_{prop} = \frac{P}{0.5\rho_\infty V_\infty^3 A_{ref}} \qquad (3)$$

The results of the RPM polar are presented in Fig. 13 for cruise conditions (M=0.82). E_{prop} corresponds to the fan power coefficient (see Equation 3). Rx corresponds to the streamwise net force coefficient (see Equation 2) including the forces on every wetted surface, the fan traction, and the OGV traction (much smaller than the fan traction but not negligible). Rx=0 means that the fan force balances the drag of the considered body, while Rx<0 means an excess of thrust.

The trends obtained with AD are confirmed by BF calculations. Those latter tend to slightly increase PSC figures at a given Rx. Indeed, while the BF predicts higher power needs for the isolated nacelle compared to the AD, an opposite behavior is observed for the BLI cases.

Some BLI-related power saving figures can be derived from Figure 13, but they strongly depend on the Rx value at which they are obtained. If every geometrical detail was included in the calculation (i.e. wings, empennage, pylon, etc) a BLI and non-BLI configuration could be compared at Rx=0 (for cruise condition). From this axisymmetric study, it is however still possible to obtain relevant data.

For instance, if the engine thrust compensates only the fuselage and nacelle drag (a configuration close to the NASA Starc-ABL configuration [10] for instance), then Rx=0. According to Figure 13, a maximum of 21% (with AD, 23% with BF) power saving on that engine could be obtained with BLI compared to an equivalent non-BLI configuration. Of course, this value concerns only the rear engine and needs to be put in perspective of the full aircraft propulsive power need. Besides, for such a low thrust level, a reduced diameter would be more relevant, thus changing the figures.

Concerning the Nautilius, although it is at this stage too early to evaluate the exact required thrust level of the full 3D concept, a tentative power saving value of 12.5% (with AD, 14% with BF) can be derived from Figure 13 looking at the high-thrust part of this curve (Rx=-100).

Another very interesting feature is the additional propulsive performance gain when going from an academic engine position to the installed configuration. It represents approximately 2% at Rx=-100 and 4% at Rx=0.

In order to better identify the power saving sources, additional calculations were performed at RPM values corresponding to Rx=-100 and Rx=0. The obtained flowfields are depicted in Figures 14 & 15.

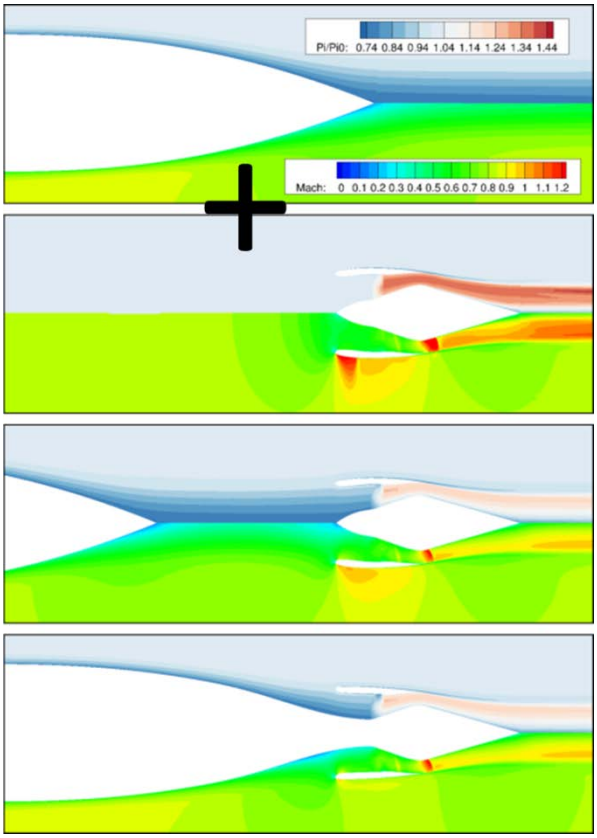

Fig. 14. Mach and stagnation pressure ratio fields corresponding to the different configurations at Rx=-100 and M=0.82, fan stage modeled via body force

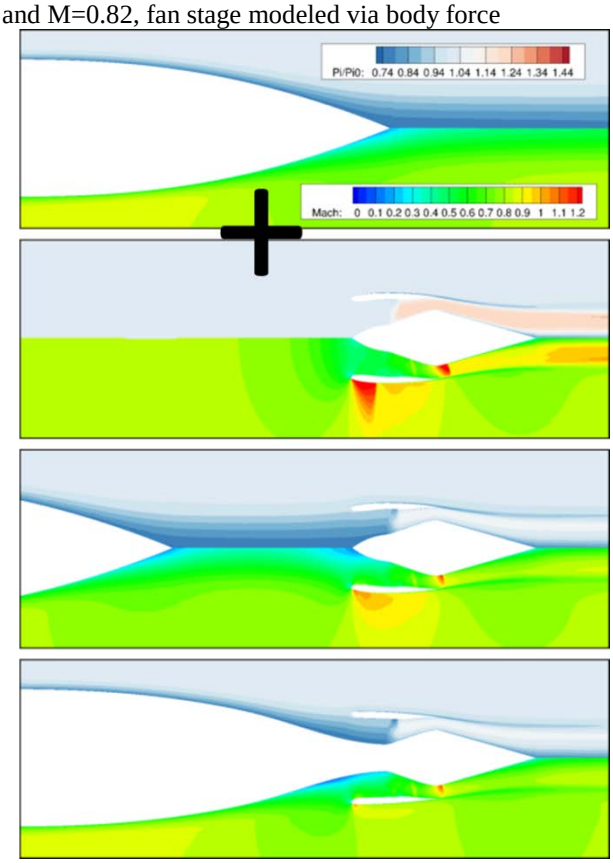

Fig. 15. Mach and stagnation pressure ratio fields corresponding to the different configurations at Rx=0 and M=0.82, fan stage modeled via body force

As the computed BLI gains are influenced by the fan stage efficiency evolutions, their values have been extracted from the computations in order to survey the AD and BF fan stage efficiency modelisation (see Fig. 16).

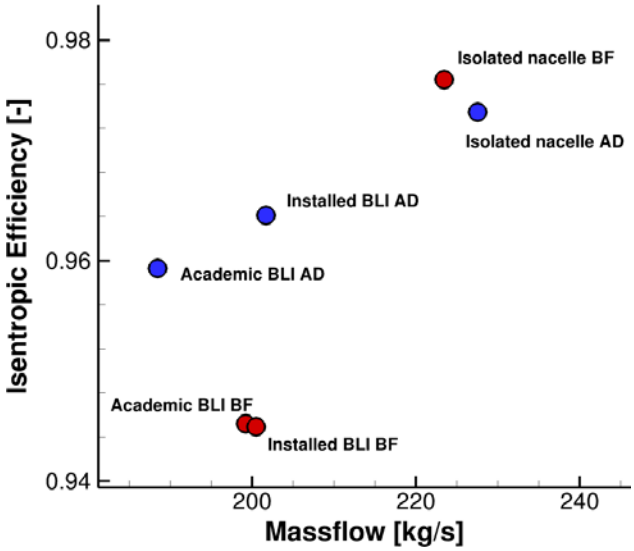

Fig. 16. Fan stage efficiency obtained with actuator disk and body force models for the different configurations at Rx=-100

While the fan stage efficiency is only marginally reduced in BLI (~ -1%) with AD, the drop is close to -4% with BF. Thus if the computations had been performed at iso - fan efficiency, the resulting BLI gains would be higher, especially with the BF model.

While the classic decomposition between drag and thrust is not relevant in the case of boundary-layer ingestion, an energy-based analysis can provide some insights on the physical phenomena at stake. The FFX ONERA in-house software [5] allows for such a breakdown based on exergy, which is the useful part of energy provided to the system that is convertible to mechanical power. The exergy balance formulation is given in Equation 4.

$$E_{prop} = W_h + E_m + E_{xth} + A_{tot} \qquad (4)$$

with E_{prop} the energy supplied to the configuration, W_h the power of the net force acting on the configuration ($R_x x V_\infty$), E_m the mechanical exergy outflow (kinetic energy and boundary pressure-work rate), E_{xth} the rate of

thermal exergy outflow and A_{tot} the anergy generation (irreversible energy loss by viscous dissipation, thermal conduction and shock waves). FFX post-processing was applied to the CFD calculations presented on Figures 14 & 15. The corresponding results are presented in Figures 17 & 18.

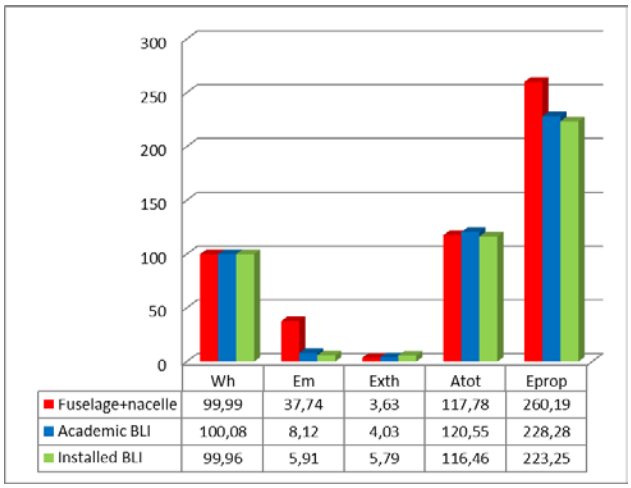

	Wh	Em	Exth	Atot	Eprop
Fuselage+nacelle	99,99	37,74	3,63	117,78	260,19
Academic BLI	100,08	8,12	4,03	120,55	228,28
Installed BLI	99,96	5,91	5,79	116,46	223,25

Fig. 17. Decomposition of terms provided by FFX post-processing tool at Rx=-100, expressed in power counts

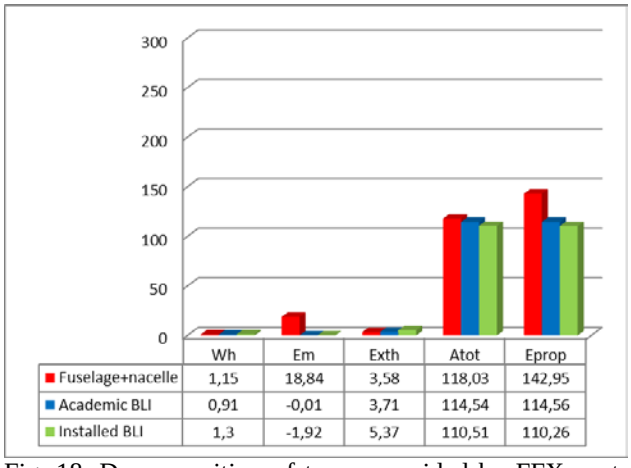

	Wh	Em	Exth	Atot	Eprop
Fuselage+nacelle	1,15	18,84	3,58	118,03	142,95
Academic BLI	0,91	-0,01	3,71	114,54	114,56
Installed BLI	1,3	-1,92	5,37	110,51	110,26

Fig. 18. Decomposition of terms provided by FFX post-processing tool at Rx=0, expressed in power counts

The terms E_m and E_{xth} represent the exergy that could be recovered in a reversible manner, while A_{tot} corresponds to the destruction of exergy in an irreversible process. All configurations are compared at the same streamwise net force, therefore W_h is constant between them. Wake and boundary-layer ingestion are both efficient ways to recover mechanical exergy. As a matter of fact, E_m was decreased by 78 to 85% at Rx=-100 and by almost 100% at Rx=0 for the BLI configurations compared to the non-BLI reference. At this stage, it is however still unclear what generates an additional BLI gain on the installed configuration compared to the academic one. To that end, a streamwise FFX analysis is performed on each configuration and presented on Figure 19.

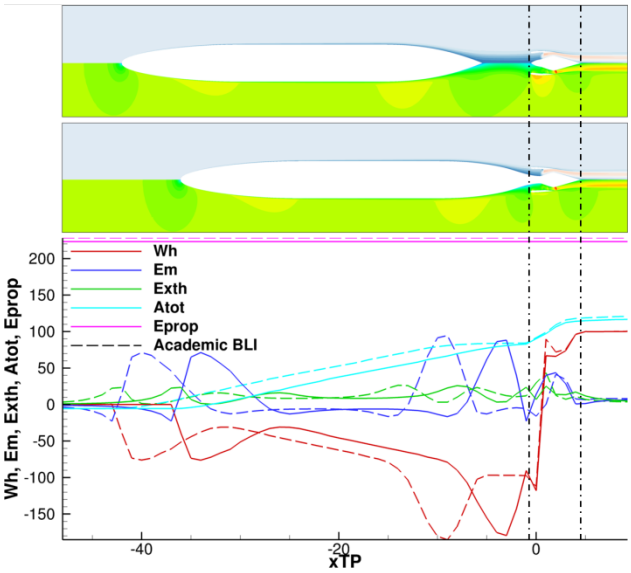

Fig. 19. Streamwise FFX decomposition on the academic and installed BLI configurations at Rx=-100

The difference can be mainly attributed to the dissipation term A_{tot}. At the air inlet entry (corresponding to the first vertical dotted black line), both configurations have destroyed similar amounts of exergy. The difference only appears in the engine region, i.e. the internal and external engine flow. Figures 14 & 15 show higher external inlet lip speeds for the academic case, which may explain at least partially the difference in the dissipation term.

5 Nautilius 3D study

As explained earlier, the main objective of this ongoing project is to evaluate the performance potential of the Nautilius concept, consisting of an aircraft with two UHBR engines integrated to the fuselage rear end. Some strong three-dimensional aerodynamic effects are expected at the airframe-to-engine interface, whose impact can only be evaluated by performing 3D aerodynamic calculations. Due to the complexity of the CAD and associated grid generation, only a limited number of parameters were investigated.

5.1 Set-up of the 3D study

Because of numerical robustness issues encountered with the Nautilius 3D configurations, another type of Actuator Disk had to be implemented. Contrary to the AD used in §4, it does not create swirl and does not use a lookup table for stagnation temperature and stagnation pressure jumps specification. In this AD version, only a uniform stagnation pressure value Pi2 downstream of the disk plane is prescribed, along with the fan polytropic efficiency η (set equal to 1 for this study). The upstream stagnation pressure Pi1 and temperature Ti1 are detected, and the downstream stagnation temperature Ti2 can be derived from Equation 5.

$$\frac{Ti2}{Ti1} = \left(\frac{Pi2}{Pi1}\right)^{\frac{\gamma-1}{\eta\gamma}} \quad (5)$$

Different values of Pi2 were imposed for each configuration in order to cover a larger thrust range. The calculations are all carried out at an AoA of 2.5°. A correction is then applied on the induced drag, and consequently on the targeted Rx value (see Equation 6), to take into account the difference between the obtained lift coefficient and the CL=0.5 target of the reference SFN configuration.

$$Rx_{corrected} = Rx + \frac{CL^2 - 0.5^2}{\pi\lambda e} \quad (6)$$

with the aspect ratio λ=12.8 and the Oswald factor e=0.875.

For geometry/grid generation simplification purposes, the empennage was not included in the calculations, as well as the nacelle support struts and fan nozzle bifurcations. It was estimated that the drag generated by those parts is counterbalanced by the missing core flow thrust. In order to be representative of a cruise condition, it was therefore judged fair to compare the configurations at Rx=0.

5.2 Reference SFN configuration

In order to be able to quantify the BLI gains, a non-BLI reference configuration is required. The NOVA SFN configuration was slightly modified to serve this purpose (see Fig. 20). The axisymmetric nacelle described in §4.2 was installed in place of the existing one, and its highlight section slightly reduced to cope with the increased speed caused by the fuselage presence. The obtained SFN configuration is free of flow separation in the conditions of interest, thus representing a proper baseline.

Fig. 20. Reference SFN configuration

5.3 Nautilius design and evaluation

The main challenge on the Nautilius configuration from an external aerodynamics point of view is to prevent flow separation in the rear fuselage region where it is divided into two separate parts. Different geometric arrangements were investigated and their impact on aeropropulsive performance quantified. In this paper two design iterations are presented, called V1 and V2, with a lateral distance effect between the two nacelles. The propulsive power requirements of these latter, obtained by CFD calculations, are compared to that of the SFN configuration on Fig. 21.

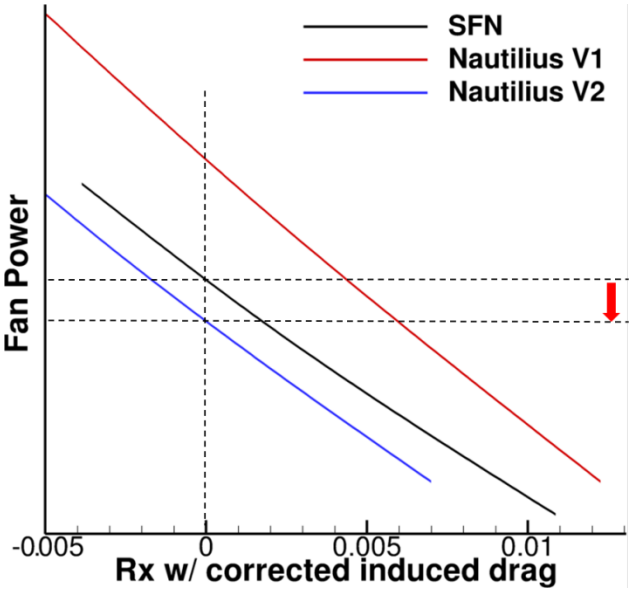

Fig. 21. Comparison of the fan power requirements calculated for the reference non-BLI configuration and for different design iterations of Nautilius, cruise M=0.82

The V1 configuration requires higher propulsive power than the SFN configuration regardless of the thrust level. A massive flow detachment is present between the separated fuselage parts and moreover the fuselage boundary layer is only partially ingested by the engines. The V2 exhibited a significant gain compared to the reference SFN configuration as the fuselage flow detachment has been considerably reduced (see Figure 22) and almost all fuselage boundary layer flow is ingested by the engines.

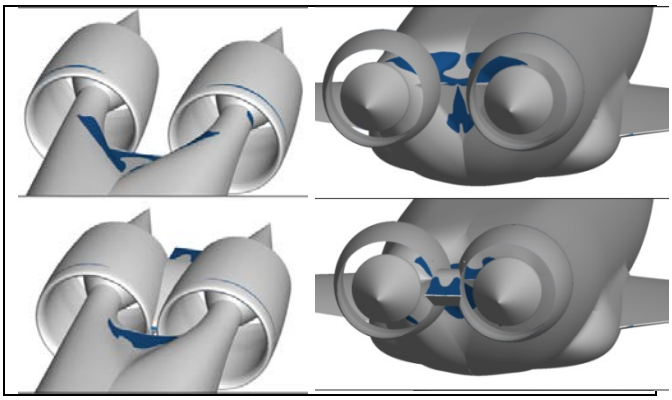

Fig. 22. Front view (on the left column) and rear view (on the right column) of Nautilius engine installation over several design iterations. From top to bottom: V1 and V2. Blue areas correspond to local flow separations.

As a matter of fact, the farther apart the nacelles, the larger the separated area. However, reducing the flow channel between the two nacelles would eventually lead to a strong nacelle interaction drag. Therefore, a "beaver tail"-like design, despite the additional wetted area it generates, was introduced on V2 to maintain the aerodynamic performance. Figure 23 illustrates the airframe/nacelles arrangement on both the V2 and SFN configurations.

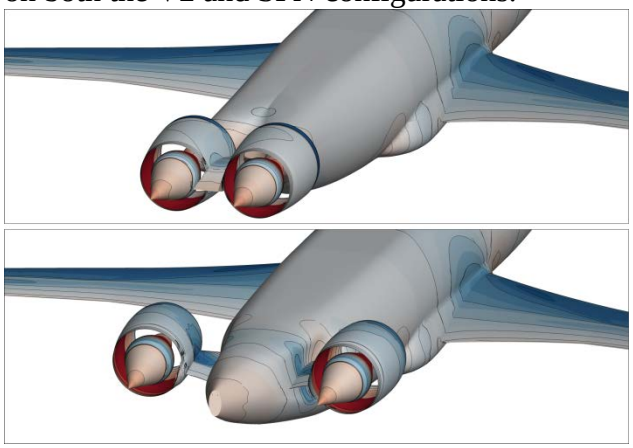

Fig. 23. Rear view of the Nautilius V2 engine installation (top) compared to the reference SFN configuration (bottom)

Conclusion and future work

The relevance of the Nautilius concept with respect to aeropropulsive performance has been confirmed by this Airbus-ONERA project. A preliminary axisymmetric CFD study helped advancing the understanding of BLI mechanisms and provided a useful baseline for the 3D design and performance evaluation. Among the next steps in this project, further design iterations based on the V2 configuration will be performed to suppress the remaining areas of flow separation in order to be able to quantify the maximum potential of the concept regarding propulsive power gains. The Body Force model used in §4 will be introduced to replace the Actuator Disk in the 3D CFD calculations to improve numerical robustness and physical representativeness. A Nautilius-dedicated fan will be designed taking into account the specific flow distortion pattern. The exploration of off-design conditions, such as take-off, landing, sideslip etc., will also be studied in order to achieve a better understanding of the highly coupled airframe-engine behavior of such a configuration.

References

[1] Negulescu, C., et al., Airbus Operations SAS Patent, Appl. Nb.: FR1655719 (2016) & US20170361939A1 (2017)

[2] Wiart, L., et al., "Development of NOVA Aircraft Configurations for Large Engine Integration Studies", AIAA Paper 2015-2254, 2015.

[3] Wiart, L., et al., "Aeropropulsive Performance Analysis of the NOVA Configurations", ICAS Paper 2016-0092, 2016.

[4] Drela, M., "Power Balance in Aerodynamic Flows", *AIAA Journal*, Vol. 47, No. 7 (2009), pp. 1761-1771.

[5] Arntz, A., "Civil Aircraft Aero-thermo-propulsive Performance Assessment by an Exergy Analysis of High-fidelity CFD-RANS Flow Solutions", PhD Thesis, Lille 1 University, 2014.

[6] Smith L. H. Jr., "Wake Ingestion Propulsion Benefit", *Journal of Propulsion and Power*, Vol. 9, No. 1, 1993, pp. 74–82.

[7] Cambier, L., Heib, S., and Plot, S., "The ONERA *elsA* CFD Software: Input from Research and Feedback from Industry," *Mechanics and Industry*, Vol. 15(3), pp. 159-174, 2013.

[8] Atinault O., Carrier G., Grenon R., Verbeke C. and Viscat P., "Numerical and Experimental Aerodynamic Investigations of Boundary Layer Ingestion for Improving Propulsion Efficiency of

Future Air Transport", *31st AIAA Applied Aerodynamics Conference*, June 24-27, 2013, San Diego, CA.
[9] Thollet W., "Body force modeling of fan-airframe interactions", PhD Thesis, 2017
[10] Welstead, J. R., and Felder, J.L., "Conceptual Design of a Single-Aisle Turboelectric Commercial Transport with Fuselage Boundary Layer Ingestion" 54th AIAA Aerospace Sciences Meeting, January 4-8, 2016, San Diego, CA.

Contact Author Email Address

ludovic.wiart@onera.fr
camil.negulescu@airbus.com

Acknowledgment

The authors would like to acknowledge William Thollet and Benjamin Godard for their assistance regarding body force approaches, Jean-Christophe Boniface for his support wrt. actuator disk calculations and Ilias Petropoulos for his help with the FFX tool.

Copyright Statement